Electronic States of Difluorocarbene Calculated by Multireference Configuration Interaction Method *

Er-Ping Sun(孙二平)[1,2**], Ting-Qi Ren(任廷琦)[2], Qi-Xin Liu(刘启鑫)[1,2], Quan Miao(苗泉)[2], Jin-Juan Zhang(张进娟)[2], Hai-Feng Xu(徐海峰)[3], Bing Yan(闫冰)[3]

[1] *College of Electrical Engineering and Automation, Shandong University of Science and Technology, Qingdao 266590*
[2] *College of Electronic, Communication and Physics, Shandong University of Science and Technology, Qingdao 266590*
[3] *Institute of Atomic and Molecular Physics, Jilin University, Changchun 130012*

(Received 3 September 2015)

We investigate the geometries and energies of seven electronic states $\tilde{X}^1A_1$, $\tilde{A}^1B_1$, $\tilde{a}^3B_1$, $\tilde{B}^1A_2$, $\tilde{b}^3A_2$, $\tilde{C}^1B_2$ and $\tilde{c}^3B_2$ of CF_2 carbene using internally contracted multireference configuration interaction methods including Davidson correction (icMRCI+Q) with different basis sets aug-cc-pVXZ (X=T, Q, 5). For the first time, the potential energy curves of electronic states of CF_2 related to the lowest dissociation limit are calculated at the icMRCI+Q/aug-cc-pVTZ level. The ab initio results will further increase our understanding of the structures and dynamics of electronic states of CF_2 radical.

PACS: 31.15.ae, 31.15.ag, 31.15.ac DOI: 10.1088/0256-307X/33/2/023101

As important reactive intermediates in many organic reactions, halocarbenes play an important role in the interstellar medium, atmospheric chemistry, gas-phase combustion reactions,[1–4] and attract much attention of experimental and theoretical studies. The long standing interest and fascination with halocarbene are due to the different reactivity and spectroscopic properties of the lowest singlet and triplet state as a result of the two nonbonding electrons occupying one or two near-degenerate orbits. In addition, the quite complicated spectroscopy and dynamics of halocarbene attributed to the typical interactions between the electronic states, for example, Renner–Teller effect, spin-orbit coupling, avoided crossing, have been a goal of published work recently (see the recent celebrated review and references therein).[5]

The difluorocarbene (CF_2), which contains the most electronegative element, fluorine, is a particularly stable species. Since the first spectral study performed by Venkateswarlu in 1950,[6] there have been extensive investigations in theory[7–12] and experiment.[13–26] *Ab initio* calculation[7–12] and high-resolution infrared spectroscopy,[17,19,21,22] laser-induced fluorescence spectroscopy,[20] electronic spectroscopy[24] have been applied to study the electronic states of CF_2. Information about the geometry, transition energy, vibrational frequency, and radiative lifetime of electronic states has been obtained.

In the past, absorption and microwave spectroscopy were used to obtain the equilibrium geometries of the lowest three electronic states of CF_2, and obtained the most accurate experimental values for the C–F bond length 1.300 Å and the F–C–F bond angle 104.94° of the ground state,[15,16,23] the bond length 1.32 Å and the bond angle 122.3° of the first singlet excited state,[16] the bond length 1.298 Å and the bond angle 118.1° of the lowest triplet state.[17] The vibrational frequencies of the ground state and the first singlet excited state were also obtained by the high-resolution laser-based spectroscopic techniques. In 1997,[27] Ma *et al.* measured the $\tilde{A} \leftarrow \tilde{X}$ spectrum by laser-induced fluorescence (LIF) excitation spectra around 250 nm and redetermined the $\tilde{A}$ state stretching frequencies $v_1 = 1012.1\,\mathrm{cm}^{-1}$ and $v_3 = 1180.2\,\mathrm{cm}^{-1}$, which were reported $v_1 = 976\pm24\,\mathrm{cm}^{-1}$, $v_2 = 496\,\mathrm{cm}^{-1}$, $v_3 = 900\pm20\,\mathrm{cm}^{-1}$ from the measurement of laser-excited single vibronic level (SVL) fluorescence spectra by King *et al.* in 1979.[20] The ground singlet state and the triplet state energy gap ($S-T$ gap) of CF_2 was measured via negative ion photoelectron spectroscopy by Lineberger *et al.* in 1999 and the value of 2.34±0.13 eV is obtained.[25]

Coincident with the development of experimental techniques, the strength of computation improved and many *ab initio* investigations have also been carried out on the CF_2 carbene giving very useful results. Most of the theoretical works are about the spectroscopic constants of the three lowest-lying states including the ground state ($\tilde{X}^1A_1$), the first excited singlet state ($\tilde{A}^1B_1$), the lowest triplet state ($\tilde{a}^3B_1$). For example, Bacskay *et al.* reported the equilibrium geometries, the transition energies, the rotational constants, harmonic force constants and frequencies of the three states of CF_2, CCl_2, CBr_2 car-

*Supported by the 2014 Postdoctoral Sustentation Fund of Qingdao under Grant No 01020120517, the Natural Science Foundation of Shandong Province under Grant No ZR2014AP001, the National Natural Science Foundation of China under Grant No 11447226, and the Scientific Research Foundation of Shandong University of Science and Technology for Recruited Talents under Grant No 2015RCJJ015.

**Corresponding author. Email: sunep1005@126.com

© 2016 Chinese Physical Society and IOP Publishing Ltd

benes using different methods in 2000.[10] Schwartz *et al.* have calculated geometries and vibrational frequencies of the singlet and triplet states of important carbenes including CF_2, and the singlet-triplet gaps, via Gaussian-2 and the QCI theory with basis sets up to 6-311+G(3*df*, 2*p*).[9] There is only one report on the states beyond the $\tilde{A}$ state, which has calculated the geometries, energies of $\tilde{X}^1A_1$, $\tilde{A}^1B_1$, $\tilde{a}^3B_1$, $\tilde{B}^1A_2$, $\tilde{b}^3A_2$, $\tilde{C}^1B_2$ and $\tilde{c}^3B_2$ of CF_2 by Cai via multireference single and double excitation configuration interaction (MRSDCI) with a triple-zeta plus double polarization (denoted as TZ+2P) basis set.[8]

Generally, most of the investigations on CF_2 are about the spectroscopic constants of the ground state ($\tilde{X}^1A_1$), the first singlet state ($\tilde{A}^1B_1$), the lowest triplet state ($\tilde{a}^3B_1$), as well as the prediction of the singlet–triplet separations. By comparison, the investigations about the higher excited states have received relatively little attention. As the numerous interactions between the electronic states, such as the Renner–Teller effect, spin-orbit coupling, avoid crossing or nonadiabatic interaction, the pre-dissociation, the spectroscopy and photodissociation dynamics are rather complicated. The information about the equilibrium geometries, the energies and the potential energy curves of the higher electronic states is needed to explain the photodissociation process in the UV range. Starting from this, our theoretical study was carried out on the equilibrium geometries, the adiabatic transition energies of seven states including $\tilde{X}^1A_1$, $\tilde{A}^1B_1$, $\tilde{a}^3B_1$, $\tilde{B}^1A_2$, $\tilde{b}^3A_2$, $\tilde{C}^1B_2$ and $\tilde{c}^3B_2$ by high-level internally contracted multireference configuration interaction including the Davidson correction (icMRCI+Q) method with different basis sets. The potential-energy curves of states correlated to the lowest dissociate limits were also studied at the icMRCI/aug-cc-pVTZ level. The calculation presented here will provide comprehensive results about the structure and behavior of electronic states of CF_2 radical.

The *ab initio* calculations on the electronic states of CF_2 carbene were carried out by using the internally contracted multireference configuration interaction (icMRCI) method[30,31] with Davidson correction (+Q).[32] The active space consists of 18 valence electrons and 12 valence orbitals (18*e*, 12*o*) corresponding to $n = 2$ atomic orbits of the C and F atom.

Firstly, the geometries and energies of seven electronic states including $\tilde{X}^1A_1$, $\tilde{A}^1B_1$, $\tilde{a}^3B_1$, $\tilde{B}^1A_2$, $\tilde{b}^3A_2$, $\tilde{C}^1B_2$ and $\tilde{c}^3B_2$ were investigated with the standard uncontracted all-electron correlation-consistent basis sets of triple, quadruple and quintuple zeta quality with polarization functions, aug-cc-pVXZ (X=T, Q, 5) and extrapolation to complete basis sets (CBS) limit.[33]

Secondly, the potential energy curves of singlet and triplet electronic states correlated to the lowest dissociation limit of CF_2 were computed by using the aug-cc-pVTZ basis set[33] with respect to the F–C–F bond angle, C–F distance, respectively. The calculations were carried out in the C_{2v} point group, when the potential energy cuts change along the F–C–F bond angle, and in the C_s point group when the potential energy cuts change along the C–F bond length. The vertical transition energy (VTE), the oscillator strength, the electron transition and the configuration were calculated in the C_s point group at the same level. The oscillator strengths are obtained from

$$f_e = \frac{2}{3}\Delta E\left|\left\langle \psi_b\left|\sum_j er_j\right|\psi_a\right\rangle\right|^2, \quad (1)$$

where the $\sum_j er_j$ is the form of the electronic dipole moment operator summed over all electrons.

All the calculations were performed using the molpro program.[34]

The optimized equilibrium geometries and the transition energies of $\tilde{X}^1A_1$, $\tilde{A}^1B_1$, $\tilde{a}^3B_1$, $\tilde{B}^1A_2$, $\tilde{b}^3A_2$, $\tilde{C}^1B_2$ and $\tilde{c}^3B_2$ states of CF_2 at icMRCI+Q level with different basis sets aug-cc-pVTZ, aug-cc-pVQZ, aug-cc-pV5Z, and extrapolations to the CBS limit, are listed in Table 1 along with the available calculations and experimental data reported in the literature.

Generally speaking, both the F–C–F bond angles and the energies increase while the C–F bond lengths decrease as the basis set is increased. As we can see from Table 1, the convergence behaviors for each geometrical parameter can be found as the increase of the basis sets. Generally, the deviation between the AVQZ and AV5Z levels is less than that between the AVTZ and AVQZ levels, indicating that the accuracy is systemically improved by using a larger basis set. Comparing our *ab initio* calculations with the experimental geometries available for the lowest-lying three electronic states, the *ab initio* structures are close to the experimental data. The C–F bond length of the ground state is quite well reproduced at the icMRCI+Q/aug-cc-pVQZ level, and has the largest divergence only 0.004 Å at the icMRCI+Q/aug-cc-pVTZ level. The C–F bond length of the first singlet excited state has the largest difference 0.006 Å at CBS and the smallest difference 0.002 Å at aug-cc-pVTZ. The bond angles are also in good agreement with the experimental data with the largest discrepancy 0.9° for the lowest triplet state. Theoretical studies about the electronic states of the CF_2 halocarbenes have been carried out by different methods, while there is only one study on the states above the $\tilde{A}$ state by Cai at the MRSDCI level.[8] Comparing different theoretical data, this work agrees with the previous calculation, with the largest discrepancy 0.1 Å and the smallest 0.001 Å of the bond lengths and the largest discrepancy 2° of the bond angle. The transition energies calculated in this work of the first excited and lowest triplet state are consistent with the experimental

results. For the transition energies of the higher states, it seems that the difference between our *ab initio* calculations and the experimental data is slightly larger. In Ref. [16], the authors pointed out that as the effect of C_2F_4 (which produced CF_2 after pulse discharge), the identification of CF_2 as the molecule responsible for the 1600 Å (7.843 eV) and 1375 Å (9.020 eV) absorption bands were tentative. Thus the experimental adiabatic transition energies of $^1A_2$ and $^1B_2$ states need further testing.

Table 1. Equilibrium geometries and energies of seven states of CF_2 calculated at the icMRCI+Q level.

CF_2	aug-cc-pvtz	aug-cc-pvqz	aug-cc-pv5z	cbs	Previous theory	experiment
			$\tilde{X}^1A_1$ state			
R_{C-F} (Å)	1.304	1.300	1.299	1.298	1.300[a]/1.299[b]/1.298[e]	1.300[c]
∠F–C–F (deg)	104.7	104.8	104.8	104.8	104.8[a]/104.8[b]/104.8[e]	104.8[c]
			$\tilde{a}^3B_1$ state			
R_{C-F} (Å)	1.317	1.313	1.312	1.311	1.317[a]/1.312[b]/1.302[e]	1.298[d]
∠F–C–F (deg)	119.1	119.1	119.0	119.1	119.4[a]/119.1[b]/119.1[e]	118.1[d]
Energy (eV)	2.462	2.474	2.480	2.481	2.42[a]/2.47[b]/2.42[e]	2.34±0.13[f]
			$\tilde{A}^1B_1$ state			
R_{C-F} (Å)	1.322	1.317	1.316	1.314	1.319[a]/1.316[b]/1.323[e]	1.32[c]
∠F–C–F (deg)	122.0	122.1	122.0	122.1	122.4[a]/122.0[b]/ 122.0[e]	122.3[c]
Energy (eV)	4.685	4.684	4.685	4.682	4.73[a]/4.67[b]/4.63[e]	4.614[g]
			$\tilde{B}^3A_2$ state			
R_{C-F} (Å)	1.546	1.539	1.537	1.535	1.5079[e]	
∠F–C–F (deg)	74.2	74.2	74.3	74.4	73.5[e]	
Energy (eV)	6.460	6.540	6.568	6.595	6.309	
			$\tilde{B}^1A_2$ state			
R_{C-F} (Å)	1.554	1.549	1.545	1.542	1.5232[e]	
∠F–C–F (deg)	73.9	74.0	74.0	74.1	73.4[e]	
Energy (eV)	6.502	6.584	6.612	6.640	6.525	7.843[c]
			$\tilde{c}^3B_1$ state			
R_{C-F} (Å)	1.566	1.560	1.558	1.555	1.5121[e]	
∠F–C–F (deg)	88.8	88.8	88.9	88.9	86.9[e]	
Energy (eV)	7.465	7.562	7.594	7.624	7.759	
			$\tilde{c}^1B_2$ state			
R_{C-F} (Å)	1.622	1.615	1.613	1.610	1.5287[e]	
∠F–C–F (deg)	87.4	87.5	87.5	87.6	85.3[e]	
Energy (eV)	7.890	8.003	8.036	8.069	9.056	9.020[c]

[a]Ref. [10], [b]Ref. [13], [c]Ref. [16], [d]Ref. [17], [e]Ref. [8], [f]Ref. [26], [g]Ref. [28].

Table 2. VTE, oscillator strength, electron configuration, and transition of electronic states of CF_2.

State[a]	VTE (eV)	Oscillator strength	Main configuration	Excitation[b]
$1^1A'(1^1A_1)$	0		$(1a'')^2(7-10a')^2(2a'')^2(11a')^2(3a'')^2(12-13a')^2$	
$1^3A''(1^3B_1)$	2.834		$(2a'')^2(9a')^2(10a')(3a'')$	$10a' \rightarrow 3a''(0.938)$
$1^1A''(1^1B_1)$	5.115	0.0389	$(2a'')^2(9a')^2(10a')(3a'')$	$10a' \rightarrow 3a''(0.897)$
$2^3A''(1^3A_2)$	8.695		$(8a')^2(1-2a'')^2(9a')(10a')^2(3a'')$	$9a' \rightarrow 3a''(0.919)$
$2^1A''(1^1A_2)$	8.778	6.06×10^{-11}	$(8a')^2(1-2a'')^2(9a')(10a')^2(3a'')$	$9a' \rightarrow 3a''(0.902)$
$1^3A'(1^3B_2)$	9.170		$(1a'')^2(2a'')(9-10a')^2(3a'')$	$2a'' \rightarrow 3a''(0.920)$
$2^3A'(2^3B_2)$	9.786		$(1a'')(2a'')^2(9-10a')^2(3a'')$	$1a'' \rightarrow 3a''(0.902)$
$2^1A'(2^1A_1)$	10.003	2.60×10^{-4}	$(1a'')^2(2a'')(9-10a')^2(3a'')$	$2a'' \rightarrow 3a''(0.828)$
$3^1A'(1^1B_2)$	10.076	0.269	$(2a'')^2(9a')^2(3a'')^2$	$(10a')^2 \rightarrow (3a'')^2(0.842)$
$3^3A'(1^3A_1)$	10.882		$(2a'')^2(9a')^2(10-11a')$	$10a' \rightarrow 11a'(0.900)$
$3^3A''(2^3B_1)$	11.197		$(6a')^2(7a')(8a')^2(1-2a'')^2(9-10a')^2(3a'')$	$7a' \rightarrow 3a''(0.871)$
$3^1A''(2^1B_1)$	11.520	0.016	$(6a')^2(7a')(8a')^2(1-2a'')^2(9-10a')^2(3a'')$	$7a' \rightarrow 3a''(0.827)$

[a]The symbol in parentheses refers to the representation of each state in the C_{2v} point group.
[b]The value in parentheses refers to the coefficient of the corresponding configuration.

As we see in Table 1, the angles of the $\tilde{A}^1B_1$ and $\tilde{a}^3B_1$ states are larger compared with those of the ground state by virtue of the removal of the electron from the in-plane sp^2-like orbital and placement in an out of-plane p-type orbital on carbon. Due to different electron transitions, which result in the change of valence shell electron repulsion and s-character of the singly occupied nonbonding orbitals, the geometries of the other four states also change compared with those of the ground state.

Potential energy curves of states correlated to the lowest dissociation limit of CF_2 are calculated with the

other two geometric parameters fixed at the $\tilde{X}$ state conformation at the icMRCI+Q/aug-cc-pVTZ level. Correspondingly, the information of the vertical transition energy, the oscillator strength, the configuration and the electron transition is also given at the same level, as listed in Table 2.

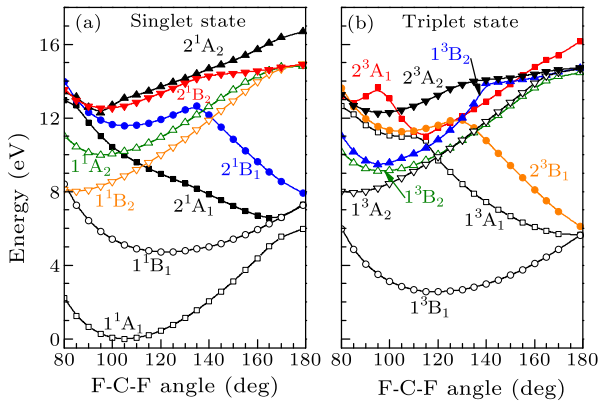

Fig. 1. Potential energy curves of CF_2 with respect to the F–C–F bond angle calculated at the icMRCI+Q/aug-ccpV(T+d)Z. The C–F bond lengths are fixed at the state equilibrium values.

The bending potential curves are displayed in Fig. 1. The calculations on the bending potential curves of CF_2 are carried out in the C_{2v} point group, and the four different representations are A_1, B_1, B_2 and A_2. As shown in Fig. 1, the ground state ($\tilde{X}^1A_1$), the first singlet state ($\tilde{A}^1B_2$), and the lowest triplet state ($\tilde{a}^3B_2$) of CF_2 carbene are bent states. The states beyond $\tilde{A}$ state, except for the 1^3A_1, 2^1A_1, 2^1B_1 and 2^3B_1 states which are considered to be linear states with the global energy minimum at ∼180°, prefer bent geometries. Different from the other CX_2 (X=Cl, Br, I)[35] halocarbene, the $\tilde{X}$ state and the $\tilde{A}$ state of CF_2 are not degenerate at the linear geometry leading to the Renner–Teller coupling between states. This means that the Renner–Teller interaction of CF_2 carbene is much less important in the accessible singlet absorption spectrum. The shapes of the bending potential energy curves for the states, which arise from the same configuration as listed in Table 2, are similar. Due to different electronic transitions, the equilibrium bond angles change significantly for different bent states, for example, the ground state 1^1A_1 has an energy minimum at about 105°, while the electronic states 1^1B_1 and 1^3B_1 with the global energy minimum at ∼130°, 1^3A_2 and 1^1A_2 at about 80°.

The C–F potential energy curves represent the dissociation

$$CF_2 \rightarrow CF(^2\Pi) + F(^2P_u), \qquad (2)$$

as illustrated in Fig. 2. The corresponding energies of the dissociation limits are 5.3 eV. The potential energy curves along the C–F bond length are calculated in the C_s point group having the two different representations A' and A''. As we can see from Fig. 2, like other halocarbenes, the lowest-lying three states $\tilde{X}^1A'$, $\tilde{A}^1A''$ and $\tilde{a}^3A''$ of CF_2 are bound states. The rest of the states above the $\tilde{A}$ state are repulsive, some of which have local minima with different dissociation barriers on their respective potential energy surface as the result of the coupling between states with the same symmetry. For example, the coupling in avoided crossing point between $2^1A'$ and $3^1A'$ states leads to the dissociation barrier in $2^1A'$ state. These repulsive potential energy cuts lead to CF+F fragments.

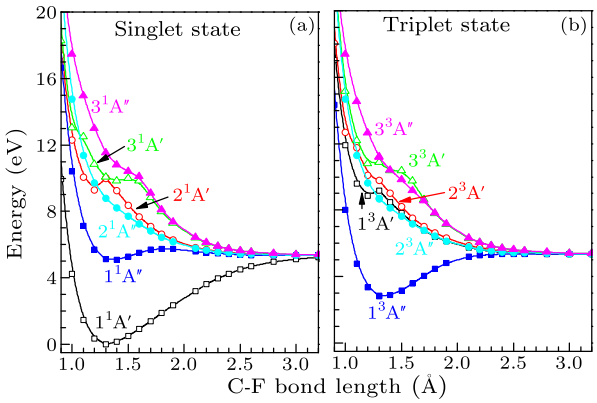

Fig. 2. Potential energy curves of CF_2 with respect to the C–F bond length calculated at the icMRCI+Q/aug-ccpV(T+d)Z. The other C–F bond lengths and the angle F–C–F are fixed at the state equilibrium values.

Table 2 lists the vertical transition energy (VTE), the oscillator strength, the electron configuration as well as the transition calculated in the C_s point group (each state was also denoted in terms of its C_{2v} symmetry and was given in brackets). The calculated VTEs of different electronic states at the $\tilde{X}^1A_1$ state equilibrium conformation are slightly higher than the adiabatic excitation energies calculated at the corresponding optimized geometry listed in Table 1. Compared with other fluorocarbenes containing the heavy atoms, CFBr[36] and CFI[37] carbenes, the state density of CF_2 is smaller in the same energy range that may be the result of the larger electronegativity of the atoms which CF_2 carbene contains.

Future work will no doubt be necessary to reveal the complicated dynamics of high excited states of CF_2 radical.

In conclusion, the equilibrium geometries, excitation energies for seven electronic states, $\tilde{X}^1A_1$, $\tilde{A}^1B_1$, $\tilde{a}^3B_1$, $\tilde{B}^1A_2$, $\tilde{b}^3A_2$, $\tilde{C}^1B_2$ and $\tilde{c}^3B_2$ of CF_2 have been calculated at the icMRCI+Q level with basis sets aug-cc-pVXZ, (X=T, Q, 5) and extrapolation to the CBS. Due to different electron transitions, the geometries of different states have large difference. Our *ab initio* structures are in good agreement with the previous experimental data and theoretical work. For the first time, the potential energy curves of the high excited state of CF_2 along the C–F bond distance and the F–C–F bond angle are examined at the icMRCI+Q/aug-

cc-pVTZ level. The vertical transition energies, the electronic configurations, and the available oscillator strengths of corresponding states are investigated at the same level.

References

[1] Wentrup C 1962 *Reactive Molecules the Neutral Reactive Intermediates in Organic Chemistry* (New York: Wiley-Interscience)
[2] Liebman J F and Simons J 1986 *Molecular Structure and Energetics* (New York: Wiley-Interscience)
[3] Finlayson P B J and Pitts J N 1986 *Atmospheric Chemistry: Fundamentals and Experimental Techniques* (New York: Wiley-Interscience)
[4] Tomioka H 2004 *Reactive Chemical Intermediates* (New York: Wiley-Interscience)
[5] Kable S H, Reid S A and Sears T J 2009 *Int. Rev. Phys. Chem.* **28** 435
[6] Venkateswarlu P 1950 *Phys. Rev.* **77** 676
[7] Staemmler V 1974 *Theor. Chim. Acta* **35** 309
[8] Cai Z 1993 *J. Phys. Chem.* **97** 8399
[9] Schwartz M and Marshall P 1999 *J. Phys. Chem.* A **103** 7900
[10] Sendt K and Bacskay G B 2000 *J. Chem. Phys.* **112** 2227
[11] Lee E P F, Dyke J M and Wright T G 2000 *Chem. Phys. Lett.* **326** 143
[12] Chau F T, Mok D K W, Lee E P F and Dyke J M 2005 *ChemPhysChem* **6** 2037
[13] Sun E, Zhang J, Li R, Sun Q, Wei C, Xu H and Yan B 2014 *Int. J. Quantum Chem.* **114** 66
[14] Laird R K, Andrews E B and Barrow R F 1950 *Trans. Faraday Soc.* **46** 803
[15] Powell F X and David R L Jr 1966 *J. Chem. Phys.* **45** 1067
[16] Mathews C W 1967 *Can. J. Phys.* **45** 2355
[17] Mathews C W 1966 *J. Chem. Phys.* **45** 1068
[18] Modica A P 1968 *J. Phys. Chem.* **72** 4594
[19] Lefohn A S and Pimentel G C 1971 *J. Chem. Phys.* **55** 1213
[20] Bondybey V E 1976 *J. Mol. Spectrosc.* **63** 164
[21] Duperrex R and Bergh H 1979 *J. Chem. Phys.* **71** 3613
[22] Hikida T, Tozawa T and Mori Y 1980 *Chem. Phys. Lett.* **70** 579
[23] Davies P B, Lewis B W and Russell D K 1981 *J. Chem. Phys.* **75** 5602
[24] Charo A and Lucia F C D 1982 *J. Mol. Spectrosc.* **94** 363
[25] Ramsay D A 1985 *J. Mol. Spectrosc.* **113** 495
[26] Schwartz R L, Davico G E, Ramond T M and Lineberger W C 1999 *J. Phys. Chem.* A **103** 8213
[27] Cameron M R, Kable S H and Bacskay G B 1995 *J. Chem. Phys.* **103** 4476
[28] Wang C, Chen C, Dai J and Ma X 1998 *Chem. Phys. Lett.* **288** 473
[29] Chau F T, Dyke J M, Lee E P F and Mok D K W 2001 *J. Chem. Phys.* **115** 5816
[30] Knowles P J and Werner H J 1988 *Chem. Phys. Lett.* **145** 514
[31] Werner H J and Knowles P J 1988 *J. Chem. Phys.* **89** 5803
[32] Langhoff S R and Davidson E R 1974 *Int. J. Quantum Chem.* **8** 61
[33] Dunning J T H 1989 *J. Chem. Phys.* **90** 1007
[34] Werner H J, Knowles P J et al 2010 *MOLPRO: a package of ab initio programs*
[35] Bacskay G B 2014 *Theor. Chem. Acc.* **133** 1474
[36] Sun E, Li R, Sun Q, Wei C, Xu H and Yan B 2012 *J. Phys. Chem.* A **116** 10435
[37] Sun E, Lv H, Shi D, Wei C, Xu H and Yan B 2014 *J. Phys. Chem.* A **118** 2447